Silicon Carbide Microsystems for Engine Applications

Robert S. Okojie
NASA Glenn Research Center
Cleveland, OH, USA
robert.s.okojie@nasa.gov

Abstract - *Several silicon carbide (SiC) pressure transducers were characterized up to 600 °C and tested under dynamic conditions. The transducer was used to validate the presence of thermo-acoustic instability at 310 Hz in a combustor test rig while operating at 420 °C and about 180 psia. Also demonstrated was the first utilization of microelectro-mechanical systems (MEMS) fabrication technology to implement a mesoscale fuel injector array platform in SiC. A combination of deep reactive ion etching (DRIE), ultrasonic micromachining, silicon sacrificial molding, and bonding of multiple SiC substrates was applied to fabricate the injector array platform. Spray patterns were demonstrated in water to determine the degree of leakage between substrates. The primary objectives of these initial efforts were: a) to develop the foundational SiC platform injector array technology for use in gas turbine engines, and b) to use such technology for mitigating thermoacoustic instabilities by active combustion control strategies.*

Keywords: Silicon Carbide, SiC, gas turbine engines, thermo-acoustic instabilities, combustion chamber, shock tube test, combustor rig test, mesoscale fuel injector array.

1 Introduction

The NASA Glenn Research Center has been developing silicon carbide (SiC) based high temperature micro sensors, actuators, active/passive platforms, and electronics aimed toward aerospace applications. This emerging technology addresses specific challenges that are associated with the development of next generation aero vehicles, which require that they burn efficiently and significantly reduce the emission of undesirable combustion by-products. NASA has a current goal to reduce nitrogen oxides (NOx) by 80% over the 1996 International Civil Aviation Organization (ICAO) standard, specifically those generated in commercial subsonic and supersonic aircraft during landing and take-off, and to reduce CO_2 by 25% relative to the 737/CFM56 engine [1]. Toward this end, we have developed SiC based piezoresistive pressure transducers that operate at 600 °C without the need for cooling (Fig. 1). These pressure transducers extend pressure measurements further into the high temperature environment than was previously possible. They would be used to: 1) support the development of suitable on-board measurement capability for flight test demonstrators, 2) monitor flight vehicle engine flow path condition, 3) verify the structural health, safety of inlet, combustor, and near nozzles, and 4) validate CFD codes for internal flows. We have also demonstrated a SiC based mesoscale, 45-fuel-injector array platform by utilizing microelectromechanical systems (MEMS) technology. The development of this new injector platform is aimed toward creating a more highly functional injector platform, compared to the current metal versions of a Multipoint Lean Direct Injector (MP-LDI) platform, which would allow for the embedding of sensors and actuators, thus eventually leading to the active control of combustion processes. The technology challenges associated with this effort, presented in subsequent sections below, include maintaining consistent form factor, bonding of multiple ceramic layers to prevent undesirable leaks, and the brazing of external metal fuel lines to the ceramic injector platform.

Figure 1. Fully packaged SiC pressure transducer fitted into National Pipe Thread housing rated to operate at 600 °C.

2 Pressure transducer development

Dynamic pressure transducers are required to measure pressure fluctuations in the combustor chamber of jet and gas turbine engines. These fluctuations may indicate an onset of thermoacoustic instabilities that could degrade engine performance. Also, the demand for lower emissions (LE) in aircraft gas-turbine engines has resulted in advanced combustor designs that are critically dependent on lean-burning (LB) operation. However, LB/LE combustors are susceptible to thermo-acoustic instabilities that can produce large pressure oscillations within the combustor. This can at a minimum disrupt compressor flow or potentially lead to premature mechanical failures. A combustor is essentially an acoustic resonator. As an engine is run through its operating range, there are states where the heat release coupling with the acoustics forms unacceptably high pressure oscillations. Such instances have been well documented [2]. This problem is expected to be more pronounced in LB/LE combustion systems because less system damping is present with LB

combustors due to reduced liner cooling. The reduced liner cooling is the result of the diversion of more cooling air to the combustion process. Traditionally this kind of problem is resolved with pre-programmed open-loop Full Authority Digital Engine (or Electronics) Control adjustments; however, there is no guarantee that such techniques can deal with all of the instabilities. Previous work to study combustor thermo-acoustic instabilities have relied upon feedback signals from pressure sensors [3]. These either were cooled or were located at some stand-off distance from the combustor, which resulted in high background noise, transport delays, as well as frequency limitation. Optical sensors potentially can give faster and cleaner signals, but they would be more effective if they could resolve the events near the fuel injectors in the combustor front-end.

Furthermore, due to the high cost that is associated with the production of future engines, designers must have as much detailed information as possible about the overall engine performance characteristics at high temperature prior to its production. Such computer-based production thus relies heavily on computational fluid dynamics (CFD) codes that are used for the engine modeling, simulation, and the extraction of the optimum engine performance parameters before they can be manufactured. Therefore, it becomes of paramount importance that the accuracy and precision of these CFD codes are physically validated by experimental results from engine tests with the utilization of robust instrumentation.

In this work, we first characterized the static pressure performance of MEMS Direct Chip Attach (DCA) SiC pressure sensors at temperatures up to 600 ^{o}C in order to extract their operating parameters. This was followed by evaluation under two dynamic conditions, one being in a laboratory shock tube with an integrated high temperature oven, and the other a combustor test rig that simulates a real engine environment [4, 5].

2.1 Transducer pre-test calibration

A static characterization of the SiC pressure transducer is usually performed to extract calibration parameters such as the zero pressure offset voltage, and full-scale output. The transducers used in these tests were rated to operate up to 600 ^{o}C and from 0-500 psi. The accelerated stress test (AST) protocol used for the static characterization has been reported elsewhere [6]. The result of the pre-test calibration in terms of the full-scale output after multiple thermal cycles is presented in representative Fig. 2. The performance characteristics of the transducer set its operational rating. The parameterized characteristics shown in Fig. 2 have been determined to be reproducible after the burn-in step of the AST as described in [6]. Therefore, they can be used for correcting the temperature induced deviations in the sensor output during data analysis. From Fig. 2, it is seen that the full-scale output becomes gradually smaller with increasing temperature. This behavior is characteristic of piezoresistive sensors commonly documented in the literature.

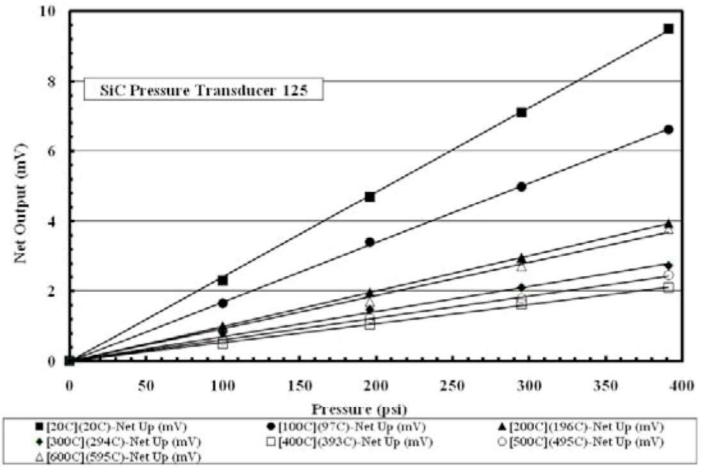

Figure 2. Full-scale net output at 400 psi of 4H-SiC pressure transducer as function of temperature.

3 Shock tube test

The shock tube uses a two-chamber tube to propagate a normal shockwave that resembles a step input to a sensor. A thin membrane separates the two chambers, one chamber with high pressure and the other with atmospheric pressure. When the membrane is pierced, a series of pressure waves are produced that coalesce into a shockwave. The shockwave produces a step response, exciting the frequency spectrum of the transducer. Pressure at the transducer is determined from analytical normal shockwave theory.

When using the sensor oven, the sensor is placed at the end of the expansion tube in line with the stagnation path of the normal shock. The transducer being tested is located at the end of the expansion tube in the sensor oven. Prior to high temperature testing, a few room temperature tests are done. The auto-spectral density is calculated from the transducer signal to see if the result is appropriate. If the results look reasonable the test is repeated several times to create an average for estimating the transfer function. This process is repeated for the desired temperature levels [4].

Each shock event needs to be windowed so that only the first shock is used in the calculations. Subsequent shocks are reflections inside the tube and have unknown excitations. A time history is produced representing a step response to the applied shock, with magnitude equal to the pressure at the sensor.

3.1 Shock tube results

The frequency and phase responses of the transducer as functions of temperature, shown in Fig. 3, revealed that the resonant frequency did not shift for the entire range of temperature tested, though the sensitivity dropped as the temperature increased, which is consistent with piezoresistive sensor characteristics. The stability of the resonant frequency at about 340 kHz was particularly significant because it indicated thermo-mechanical stability within the sensor/package system and stability of the sensor bandwidth across the range of operating temperature.

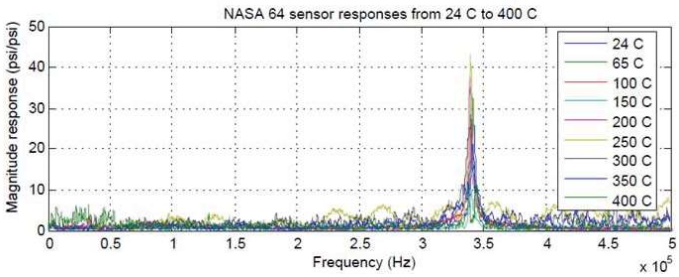

Figure 3. Frequency response of SiC pressure transducer as function of temperature during shock tube test [4].

4 Combustor rig test

Another previously characterized SiC pressure sensor was used to demonstrate survivability in the high temperature and high vibration engine environment by testing it in a combustor test rig, with output compared against the facility pressure transducer. Thermo-acoustic instabilities were measured at 420 ^{o}C and at pressures up to 180 psi in an experimental test rig shown in Fig. 4 [5]. The pressure transducer was inserted and locked into a pressure port plug as shown. The ease of insertion into the combustor pressure port plug is due to the tubular design of the sensor sub-package that allows for flexible insertion into any engine pressure port plug (e.g., a borescope plug) that can receive the package outer diameter of 0.25 in.

4.1 Combustor test results

Following the pre-test calibration, the SiC transducer was inserted into the combustor test rig by screwing the pressure port plug, now with the sensor, into the location shown in Fig. 4, where temperature could reach as high as 450 ^{o}C during operation. The response of the SiC pressure transducer (P3MEMS) was then compared with the facility reference transducer (P3) and a water-cooled piezoceramic transducer (PSP001) that was located upstream in the rig. At ignition, at which the highest temperature was recorded (420 ^{o}C), the SiC sensor strain sensitivity resulted in lower output relative to P3. However, the SiC output signal to noise ratio was sufficient to detect thermo-acoustic instability. Fig. 5 compares the high frequency response of P3MEMS to PSP001 during the combustion process. The amplitude spectral density and brief time history from time of ignition shown in Fig. 5 reveal the existence of thermo-acoustic instability at 310 Hz as detected by the P3MEMS. This was in excellent agreement with that obtained by the reference sensor PSP001.

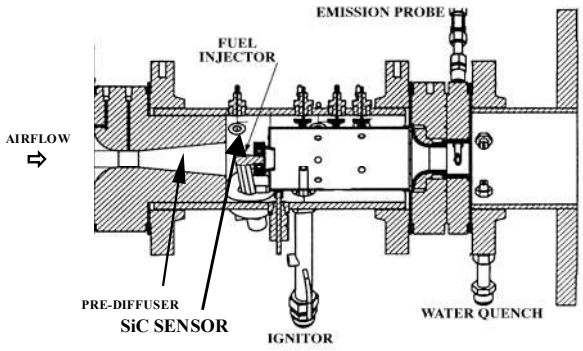

Figure 4. Test rig designed to replicate real instability at engine conditions. Location of the SiC pressure sensor relative to the combustion chamber is shown.

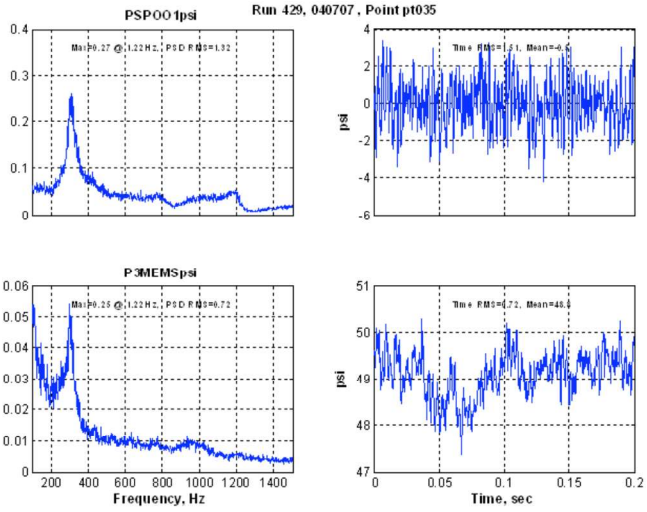

Figure 5. Amplitude spectral density (left column) and brief time history (right column) for the commercial piezoelectric pressure transducer (PSP001) and the SiC pressure transducer (P3MEMS) show the detection of thermo-acoustic instability at 310 Hz by both devices.

5 SiC mesoscale lean direct injection

The metal versions of a Multipoint Lean Direct Injector (MP-LDI) array offered promising results in reducing NOx as shown in Fig. 6 [7]. However, metal MP-LDIs suffer from the following: warpage due to creep and fatigue after a short combustion operation; the electrochemical etching used to form the flow channels in metal typically leaves curved corners as opposed to the originally designed sharp corners, thereby changing the flow profile; rough surface morphology after electrochemical etching of the channels impedes the flow of fuel and causes undesirable turbulence; and because of the high surface energy of the metal, coking

of the fuel occurs at the operating temperature that leads to clogging of the injectors.

For the purpose of performing intelligent control of combustion to monitor, predict, and control or mitigate the potential for lean blow out (LBO) and reduce combustion instabilities, the next generation of aerospace vehicles will preferably require proximal active control of the combustion chemistry. The chemistry associated with combustion results in undesirable products such as NOx, CO, and hydrocarbons, thermo-acoustic instabilities, and noise generation. The most desirable solution strategy will be to have distributed actuators and sensors (pressure, temperature, and chemical) to be as close as technologically possible to the combustion source. This will allow for improved response time to sense the onset of the precursor conditions for LBO, and provide timely control to return back to normal combustion.

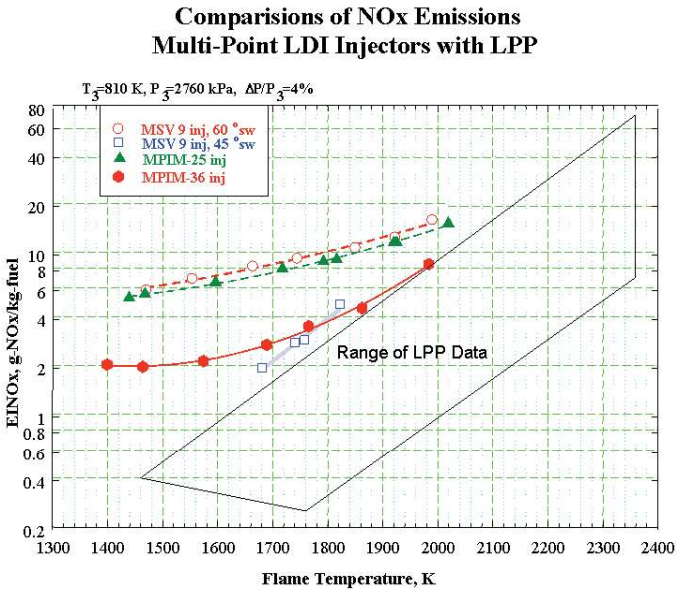

Figure 6. Comparison of flame-tube NOx emission from metal MP LDI configurations from 9 to 36 injector array. It shows significant NOx reduction with increasing injector array [7].

In this work, we report the initial step towards the development of a SiC based active combustion control system by demonstrating the SiC version of the MP-LDI platform utilizing advanced micromachining techniques such as DRIE, ultrasonic machining, and loss molding. It is the objective of this effort to eventually integrate the SiC-based sensors, actuators, and electronics to the SiC MEMS MP-LDI array platform. This is with the ultimate goal of implementing active control of local fuel-air ratio in the combustor to reduce NOx emissions and thermo-acoustic instabilities.

5.1 Injector array description

A schematic cross section diagram of the SiC MEMS MP-LDI, shown in Fig. 7, depicts the concept. It is comprised of a fuel plenum that holds the fuel volume while isolating the fuel from air (SEM image shown in Fig. 8a), the inlet that takes fuel from the plenum and initiates the swirl action (Fig. 8b), the cascaded fuel swirl chamber that creates turbulence, and the injector orifice (Fig. 8c). The air swirl section is next, where fuel and air mix to increase fuel break up into smaller particle diameters, thereby increasing burn efficiency (Fig. 9).

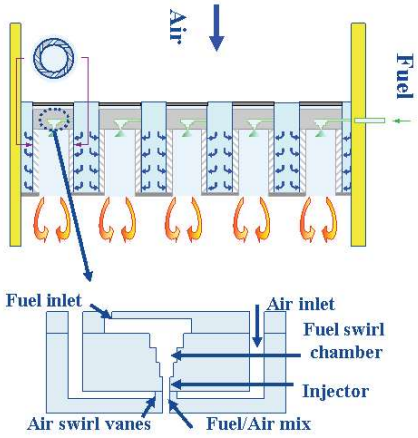

Figure 7. Cross section drawing of the SiC MP-LDI showing air and fuel swirlers and injector sections. Notice the interaction between fuel and air occurs only at the mixing stage inside the air swirl chamber, just prior to burn.

An isometric view showing the model stack of SiC substrates is presented at the top right section of Fig. 10. The fabricated SiC substrates are shown in the middle of the figure prior to bonding. This figure also shows the demonstrated spray pattern after bonding and testing (see bottom right of figure). The bottom left section of the figure shows a magnified view of the air swirl chamber that reveals the angular arrangement of the vertically slotted vanes. This arrangement provides the angular momentum force required for the air to shear the fuel that is swirling out of the injector orifice and traversing the air swirl chamber. The fuel swirls in a counter rotating direction to the air so further fuel break-up into small droplets can be accomplished.

Fabrication of the fuel plenum, fuel inlet, and cascade fuel swirl chamber/injector orifice substrates was accomplished by the combination of ultrasonic machining and DRIE, with depths ranging from 200 μm for the injector orifice to 2 mm for the plenum. The angled air swirler vane, which is 6.35 mm high, was fabricated using the silicon loss-mold technique. This was accomplished by the DRIE of the air swirler negative image in silicon, followed by the chemical vapor deposition of SiC.

Planarization was performed by lapping and polishing. Finally, the silicon was selectively dissolved in an equal mixture of 49% HF and HNO_3 to release the SiC air swirler. Bonding of the SiC substrates was accomplished by the sputter deposition of 10 μm titanium on the surfaces to be bonded, followed by the application of 75 μm high temperature glass tape. The substrates were then heated to 1200 °C to allow diffusion reaction between the titanium and glass tape.

To determine the bond strength, a four-point bend test based on the ASTM 1161 standard was performed on bonded test specimens [8]. The average flexural strength and shear strength obtained were found to be about 700 MPa and 25 MPa, respectively. These were significantly higher than the maximum fuel pressure of 2 MPa at the main fuel line, thereby assuring that premature separation would not occur. The main 2 MPa fuel line, shown in the top left of Fig. 10, is made of kovar tube, which splits into four tubes which are inserted into holes in the SiC plenum and brazed into place. These lines supply fuel to the plenum.

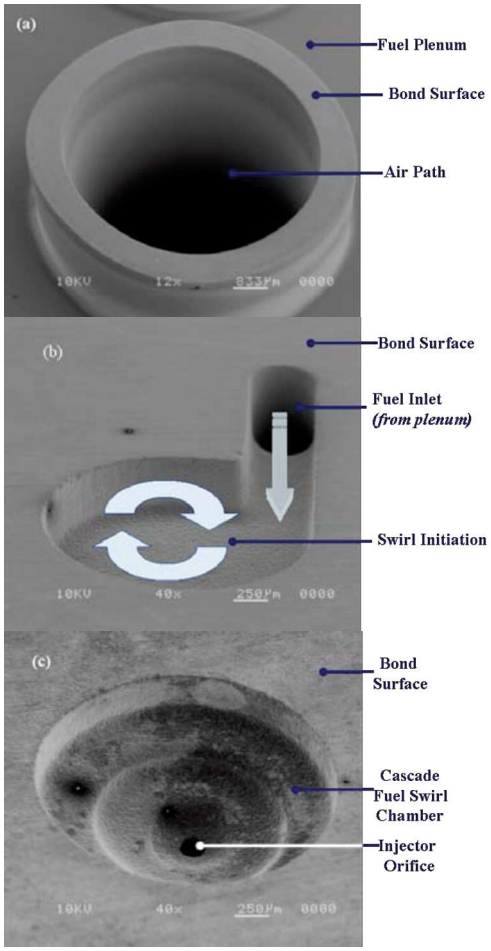

Figure 8. SEM images of SiC substrates which comprise a) fuel plenum, b) fuel inlet that feeds the fuel swirl chamber and c) the fuel swirl chamber with the injector orifice.

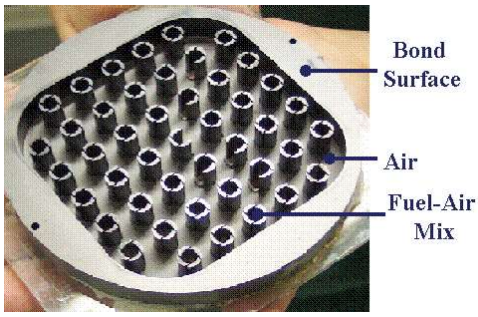

Figure 9. Optical image of the air swirl chamber where fuel and air would mix to induce fuel break up into smaller particle diameters.

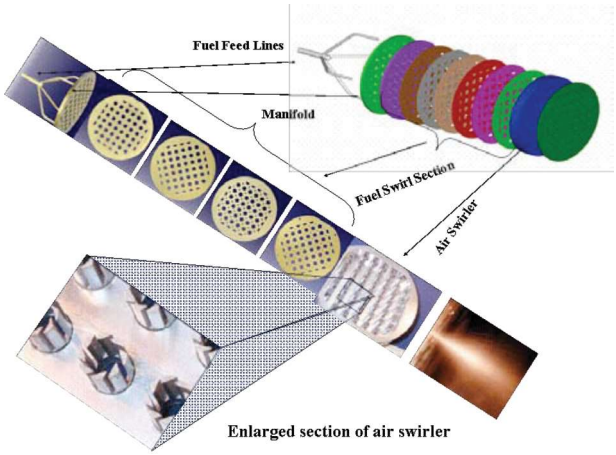

Figure 10. Isometric view of the conceptual model showing the SiC stack (top right), the corresponding fabricated substrates with their various functions (middle), and the magnified air swirl chamber (bottom left).

5.2 Preliminary test results

The preliminary results of this initial test are limited to observation of the pre-mix and mix spray patterns and also the degree of leakage at the Kovar/SiC joints and the substrate bond lines. The pre-mix spray pattern is shown in Fig. 11a (without the air swirler), which shows a uniform water stream pattern from the injectors. With the air swirl section attached, a dramatic improvement in the atomized spray was observed, with a mean particle diameter of approximately 50 μm by flow visualization (see Fig. 11b).

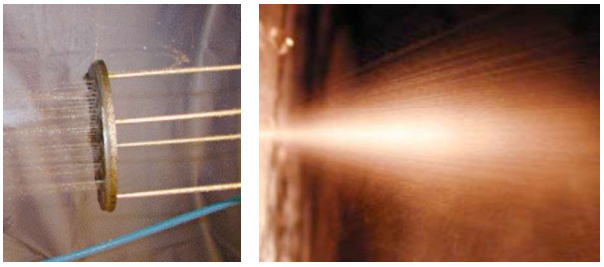

(a) (b)

Figure 11. a) Completed SiC MEMS MP-LDI array shows uniform spray pattern, and, b) atomized spray pattern after mixing.

This preliminary result confirmed the effectiveness of the air swirler to create break-ups. Further characterization of the flow pattern using fuel both cold and during combustion will be pursued. Leakage was observed at the plenum/inlet bond line. Analysis showed that the leakage was due to the presence of an area that was free of bond material.

6 Conclusions

The ability of un-cooled MEMS-DCA packaged SiC pressure transducers to be used for the sensing of dynamic pressure fluctuations in a combustion chamber has been demonstrated. A shock tube test indicated that the transducer has a high resonant frequency that is well above the frequencies that are associated with thermoacoustic instabilities in the combustion chamber of gas turbine engines. Because the SiC transducer is inserted directly into the sensed environment, real time accurate readings are obtained, thus leading to a more accurate validation of the CFD codes used for engine modeling. We presented the preliminary results of the utilization of a combination of DRIE, ultrasonic machining, and silicon loss molding techniques to fabricate a 45- injector array platform in SiC. The preliminary result with water demonstrated spray atomization.

Acknowledgments

The SiC pressure sensor and MP-LDI tasks were initially funded under the NASA Ultra Efficient Engine Technology and Smart Efficient Component Projects, respectively. They are currently funded under the Subsonic Rotary Wing and Subsonic Fixed Wing Projects under the Fundamental Aeronautics Program. We thank the technical staff of the NASA Glenn Combustion Branch and Controls and Dynamics Branch for their support. We specially thank Professor Mitch Wolff and his students at the Wright State University for the shock tests.

References

[1] F. Collier, E. Zavala and D. Huff, NASA Fundamental Aeronautics Program, "Subsonic Fixed Wing Project," NASA Reference Document, http://www.aeronautics.nasa.gov/nra_pdf/sfw_proposal_c1.pdf, Accessed: 10/28/2009.

[2] A.H. Lefebvre, *Gas Turbine Combustion*, 2nd Edition, Taylor & Francis, Philadelphia, PA, 1999.

[3] J.C. DeLaat and C.T. Chang, "Active control of high frequency combustion instability in aircraft gas-turbine engines," Proc. 16th International Symposium on Air-breathing Engines, Cleveland, OH, Paper No. ISABE-2003-1054, NASA TM-2003-212611, Aug.-Sept. 2003.

[4] R.S. Okojie, S.M. Page and M. Wolff, "Performance of MEMS-DCA SiC pressure transducers under various dynamic conditions," Proc. IMAPS International High Temperature Electronics Conference, Santa Fe, NM, pp. 70-75, May 2006.

[5] R.S. Okojie, J.C. DeLaat and J.R. Saus, "SiC pressure sensor for detection of combustor thermoacoustic instabilities," Proc. 13th International Conference on Solid-State Sensors, Actuators and Microsystems, Seoul, Korea, June 2005.

[6] R.S. Okojie, E. Savrun, P. Nguyen, V. Nguyen and C. Blaha, "Reliability evaluation of direct chip attached SiC pressure transducers," Proc. IEEE Sensors Conference, Vienna, Austria, pp. 635-638, Oct. 2004.

[7] R. Tacina, A. Mansour, L. Partelow and C. Wey, "Experimental sector and flame-tube evaluations of a multipoint integrated module concept for low emission combustors," GT-2004-53263, ASME Turbo Expo 2004: Power for Land, Sea and Air Conference, Vienna, Austria, June 2004.

[8] ASTM International, "Standard test method for flexural strength of advanced ceramics at ambient temperature," ASTM Standard C1161-90, West Conshohocken, PA, pp. 329-335, 1990.